

The influence of a single quantum dot state on the characteristics of a microdisk laser

Z. G. Xie,¹ S. Götzinger,² W. Fang,³ H. Cao,³ and G. S. Solomon^{*,2,4,5}

¹*Department of Applied Physics, Stanford University, Stanford, CA 94305, USA*

²*Edward L. Ginzton Laboratory, Stanford University, Stanford, CA 94305, USA*

³*Department of Physics & Astronomy, Northwestern University, Evanston, IL 60208, USA*

⁴*Solid-State Photonics Laboratory, Stanford University, Stanford, CA 94305, USA*

⁵*Atomic Physics Division, NIST, Gaithersburg, MD 20899-8423 USA**

We report a quantum dot microcavity laser with a cw sub- μ W lasing threshold, where a significant reduction of the lasing threshold is observed when a single quantum dot (QD) state is aligned with a cavity mode. The quality factor exceeds 15 000 before the system lases. When no QD states are resonant, below threshold the cavity mode initially degrades with increasing pump power, after which saturation occurs and then the cavity mode recovers. We associate the initial cavity mode spoiling with QD state broadening that occurs with increasing pump power.

PACS numbers: 78.67.Hc, 42.55.Sa, 78.45.+h, 78.55.Cr

While the first masers and lasers were demonstrated in gas and solid-state systems, respectively, the scaling of masers [1] and lasers [2] to a small number of emitters has been investigated for two decades using atomic emitters, such that recently a one-atom laser has been demonstrated [3]. These systems feature external cavities where the atom is typically strongly coupled to the radiation field, and require ultra-high vacuum chambers. Recently, approaches are combining microcavities and atomic emitters [4]; however, they are difficult to implement and are not monolithic.

Semiconductor-based lasers are compact, intrinsically monolithic, and ubiquitous, but a single-emitter laser, an analog to the single atom laser, has not been observed. Typical devices are pumped nonresonantly through carrier transport and employ heterostructures, often with active regions of reduced dimensionality. An active medium of QDs provides an ensemble of sharp excitonic states for lasing [5], and was demonstrated using a dense ensemble of QDs in 1994 [6]. If the QD distribution is made dilute so that only a few discrete QD states are present, extremely low threshold lasers can be made provided the photon storage time is adequate to ensure stimulated emission. Such a system is a promising route to solid-state, single-emitter lasing.

QD microdisk lasers have been reported [7, 8], with thresholds of 5-20 μ W. In these devices many QDs are randomly distributed and thus most are at best weakly coupled to the cavity mode unless additional techniques are used to align the emitter and cavity mode [9, 10, 11]. For single-emitter devices, the number of coupled emitters can be decreased by reducing the cavity size or by using crystal growth techniques that increase the QD spectral distribution and reduce the overall density. Single QD emission can be coupled to micropillars [12], microdisks [13] and 2D photonic crystal cavities [14]. The mode volume in microcavities can be reduced to a few cubic wavelengths, with cavity Q 's exceeding 10,000 [15, 16, 17, 18, 19]. Here,

we demonstrate a QD microdisk laser with thresholds in the 500 nW range on 1.8 μ m diameter disks with a cavity Q exceeding 15 000 at threshold. While the lasing process likely involves many emission states, the tuning of a single QD emission state through the cavity alters the lasing threshold by a factor of approximately 3.

Our samples are grown by molecular beam epitaxy. The structure contains an initial GaAs layer of 300 nm on a GaAs substrate, followed by 700 nm of $\text{Al}_{0.8}\text{Ga}_{0.2}\text{As}$, 75 nm of GaAs, InAs QDs, and 75 nm of GaAs. The QD density is approximately 50 QDs/ μm^2 . Microdisks are fabricated with standard photolithography and an isotropic wet chemical etch to define an initial post, after which a HCl-based selective etch is used to undercut the AlGaAs. For photoluminescence (PL) measurements, the sample is mounted in a continuous-flow helium cryostat. A 0.75 NA objective lens is used to collect PL emission from the microdisk sample. A Ti-sapphire laser operating cw or mode locked was used to excite the QDs nonresonantly through the same objective lens. Unless otherwise noted, measurements were conducted at 7 K with 780 nm cw laser excitation. Under these conditions, carriers are created in the GaAs, diffuse and relax through wetting layer states, and into QD states. The QD emission is fiber-coupled to either a spectrometer, a spectrometer-streak camera for wavelength-selective time-resolved measurements, or a second-order correlation setup for photon statistics measurements. The beam diameter of the pump can be adjusted at the sample from 1.5 to 8.5 μ m.

PL was first measured from a nonprocessed planar region of the sample with a large beam size (8.5 μ m) and an excitation power density of 2.5 W/cm². With this spot size, there are approximately 3000 QDs illuminated. PL from this region is shown in Fig. 1(a). We observe broad, ensemble QD emission centered around 905 nm. Similar measurements were done on the disk sample and are shown in Figs. 1(b) and 1(c). However, because of the small disk areas and hence the small number of illu-

minated QDs, the PL spectra show much sparser overall emission with the presence of discrete emission states. Second-order correlation measurements show that these states are typically antibunched. Microcavity whispering-gallery modes are observed in both figures. The free spectral range of the cavity is approximately 45 nm in the vicinity of the QDs emission, and thus two modes are typically observed. One of the modes (mode L) is located at the long-wavelength side of the QD distribution, while the other (mode S) is located at the short-wavelength side. In most of our cavities here is a mode splitting of 0.2 nm (300 meV) [as seen in Figs. 1(b) and 1(c)] of the ideally degenerate counterpropagating modes. The splitting is due to coupling of the modes through surface defects or other symmetry breaking in the microdisks. We identify these as either the long or short wavelength branch of the mode.

We typically observe cavity mode lasing in S but not in L, likely due to the distribution of states, as seen in Fig. 1(a). Results of laser pump-power versus intensity (L-I) measurements on a 1.8 μm diameter disk are shown in Figs. 2(a) and 2(b) for the long-wavelength branches of modes S and L. For mode S, as we increase the excitation power we first observe a modal linewidth increase from approximately 0.05 to 0.16 nm (245 μeV), then a linewidth decrease to the spectrometer resolution limit of 0.036 nm (55 μeV). The decrease of the modal linewidth with increasing pump power is attributed to a gradual

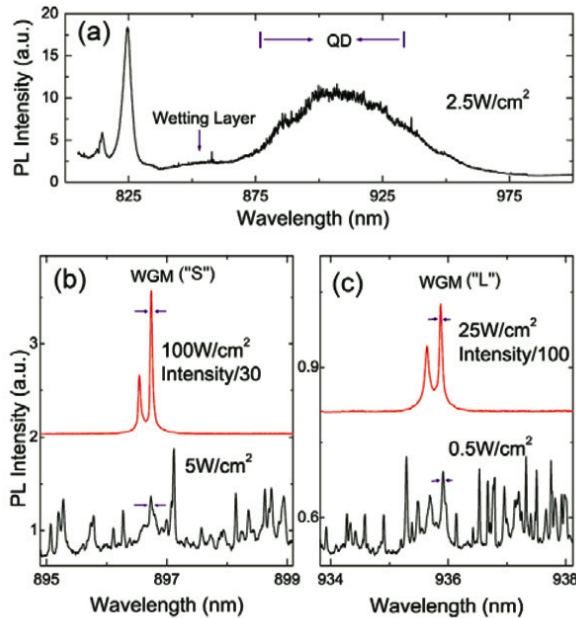


FIG. 1: (a) PL spectrum from an unprocessed region at 7 K under low excitation, showing QD emission. (b) PL spectra on a 1.8 μm diameter microdisk near cavity mode S, for two different excitation powers. (c) On the same disk, the PL spectra near mode L, for different excitation powers.

saturation of absorbing states and the onset of stimulated emission. We performed the same measurement on the long-wavelength side of mode L. A similar trend is seen in the linewidth evolution; however, both the initial modal linewidth broadening and the following decrease are much smaller, and most significantly, the eventual linewidth levels off at 0.06 nm, well above the spectrometer resolution. The L-I curves shown in Fig. 2(b) suggest a soft lasing transition for mode S, as would be expected for high spontaneous emission coupling observed in microcavities [20]. The transition to lasing is confirmed in the microdisks through second-order correlation measurements, [Fig. 2(c)] where bunching is observed around the threshold and Poissonian photon statistics are observed well above threshold [21, 22, 23]. For comparison, the L-I curve for mode L has a nearly linear dependence until the QD states saturate, indicating the absence of lasing. In comparing the above data we conclude that the trans-

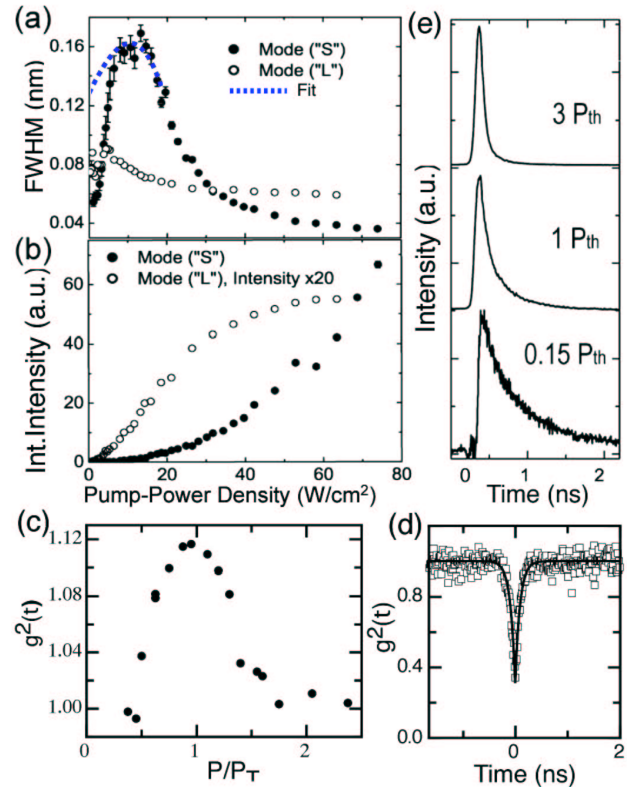


FIG. 2: (a) Evolution of the linewidth of the long-wavelength branches of modes S and L shown as a function of pump power. The lasing threshold is at a power density of 30 W/cm^2 ; broken line is theory. (b) The cavity mode integrated intensity change with pump power shown for S and L; L saturates before the onset of lasing. (c) Second-order correlation measurements [$g^2(\tau)$] for various pump powers. (d) $g^2(\tau)$ in the weak excitation limit on a QD state separated from the mode indicating antibunching (no background or dark count correction). (e) Time-resolved PL measurements show the reduction of the lifetime associated with stimulated emission from mode S.

parency window is reached at a pump-power density of 30 W/cm² for S, corresponding to a 750 nW threshold for this microdisk.

The initial broadening of the modal linewidth in Fig. 2(a) is related to increasing absorption: with increasing power the QD states broaden, resulting in enhanced spectral overlap with the cavity mode and enhanced absorption. At low pump power, the linewidth of the QD states are typically below the spectrometer resolution. The isolated emission usually shows antibunching in the second-order correlation function, as is expected from a single anharmonic quantum system. An example is shown in Fig. 2(d). However, at threshold the states can broaden to approximately 0.13 nm (200 μ eV).

To observe the dynamical behavior we have made wavelength-selective time-resolved measurement on S. The sample is probed with pulsed 850 nm laser light, in the vicinity of the InAs wetting layer to reduce the carrier relaxation time to the QD states. Under this condition the absorption coefficient is roughly 20 times lower. A selection of our pump power results is shown in Fig. 2(e), where the emission is on resonance with cavity mode S. At a low pump power, the time-resolved intensity curve shows the emission decay of excitons with a lifetime of \sim 500 ps. With increasing pump power, the measured lifetime decreases, and finally reaches a decay time of 47 ps. Since we observe a rise time of \sim 50 ps due to carrier diffusion to and relaxation into the QD states, the 47 ps decay time is now determined by a combination of the carrier capture processes, the lifetime, and our \sim 20 ps temporal resolution.

From statistics, we expect 130 QDs inside the disk plane and approximately 60 QDs spatially located in the cavity mode region, which extends \sim 250 nm into the disk plane from the edge. On average, the number of QD states spatially and spectrally coupled to the cavity resonance at low excitation power is much less than unity. However, the actual spectral coupling near the lasing threshold is determined by the homogenous broadened linewidth of the QD emission.

To clarify the modal linewidth broadening and lasing with the apparent absence of an aligned QD state we suppose there are several QD states in the spectral vicinity of the cavity mode, each with average occupancies N_i , where $0 \leq N_i \leq 1$ for each QD state i . If we assume that states from different QDs do not interact, a general description of the net stimulated emission or absorption is $\sum_i \beta_i \dot{g}_i (N_i - \frac{1}{2})$, where g_i is the coupling factor between the i th QD state and cavity mode, and g_i is the stimulated emission (absorption) coefficient for the i th state. Because the spatial and polarization alignments of the cavity mode and each QD state i are constant, β_i is equivalent to the spectral coupling factor modified by a constant, and is $\beta_i = \alpha_i \int f(\lambda - \lambda_0, \Delta\lambda_0) h(\lambda - \lambda_i, \Delta\lambda_i) d\lambda$, where $f(\lambda - \lambda_0, \Delta\lambda_0)$ is the spectral distribution of the cavity

mode, $h(\lambda - \lambda_i, \Delta\lambda_i) d\lambda$ is the spectral distribution of the i th state, and α_i is a constant. λ_0 and λ_i are the wavelengths of the cavity mode and i th state, and $\Delta\lambda_0$ and $\Delta\lambda_i$ are their respective linewidths. Assuming Lorentzian distributions for f and h , $\beta_i \propto \pi^{-1} (\Delta\lambda_0 + \Delta\lambda_i) \times [(4\lambda_0 - \lambda_i)^2 + (\Delta\lambda_0 + \Delta\lambda_i)^2]^{-1}$. Since we observe that $\Delta\lambda_i$ is pump-power dependent, β_i will be as well. Below transparency, $\Delta\lambda_0 \propto \sum_i g_i \beta_i (N - \frac{1}{2})$. To estimate

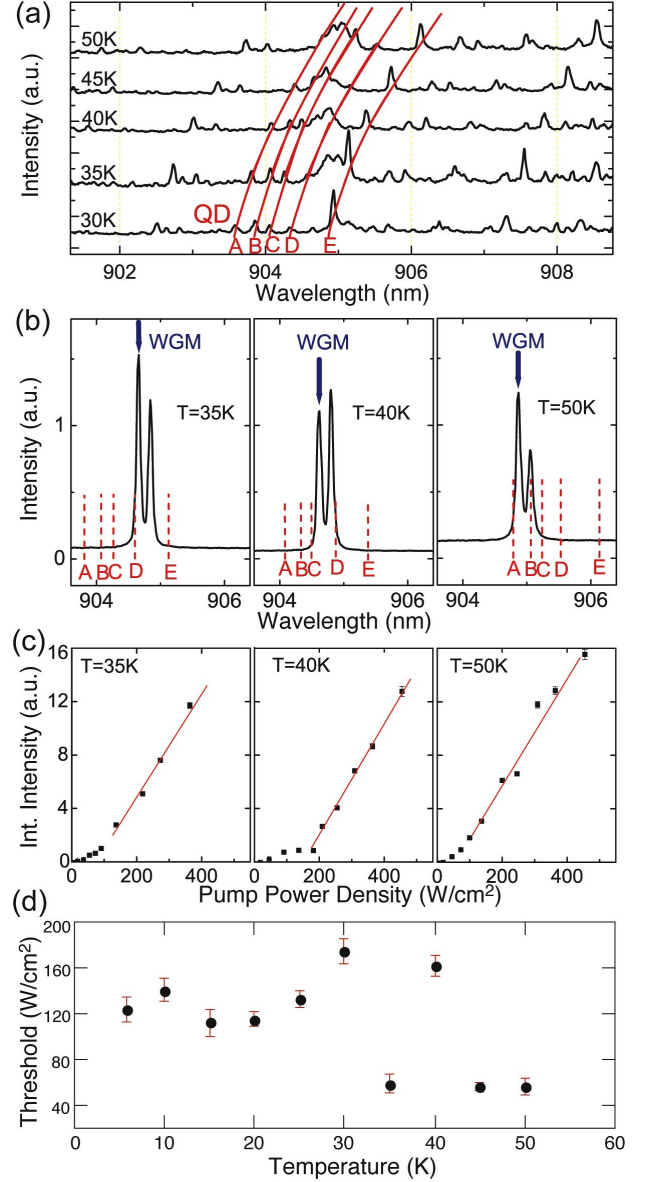


FIG. 3: 1 (a) PL spectra of QD emission and mode position at different temperatures. Between 35 to 50 K, QD lines A, B, C, and D cross the cavity modes. Lines are guides following QD emission shifts. (b) The PL spectra show the spectral alignment of QD A, B, C, and D (under weak excitation) with mode S at high excitation. At 35 K D is aligned and at 50 K A is aligned with the short-wavelength branch of the split mode. (c) The L-I curves at 35, 40, and 50 K. Lines are guides. (d) Lasing thresholds at various sample temperatures.

the change in $\Delta\lambda_0$ with pump power, we assume only the emitters nearest the cavity mode couple, and use the average nearest neighbor emitter modal detuning, with a detuning taken from experimental data (~ 0.25 nm). We use a value for $\Delta\lambda_i$ at threshold taken from the data (0.13 nm) and assume a sublinear excitation dependence [24]. Finally, we assume N_i varies linearly with pump power below transparency. Then, the modal linewidth variation can be determined with only a scaling factor as a free parameter. This is shown as a broken line in Fig. 2(a), and accurately represents the linewidth broadening. Thus, when QD states are present and subject to power broadening, but are initially only weakly overlapping with the cavity, we can expect the modal linewidth to increase below transparency. Furthermore, the system can lase at higher powers if the cavity Q is adequate. Now, we contrast this to the situation when a QD state is aligned with the cavity mode.

Because the refractive index change with temperature is much smaller than the bandgap change with temperature, the QD emission lines can be tuned through the cavity modes by adjusting the sample temperature. In most of our samples lasing persists when the sample is tuned from 6 to 55 K (a QD tuning range of 1.5 nm). This indicates the lasing is not based exclusively on observable QD states resonantly coupled to the mode [23]. However, the relative spectral tuning of observed QDs emission states and cavity modes does influence the L-I curve. In Fig. 3(a), we show the position of cavity modes and QD emission peaks when the sample is temperature tuned under low pump power. At 35 K the QD emission line D crosses the cavity mode, and at 50 K the QD emission lines A and B also cross the mode. Because the QDs are randomly distributed throughout the disk, spectral alignment between the cavity mode and QD state does not guarantee coupling. We show spectra and L-I measurements for the short-wavelength branch of mode S at three different sample temperatures, 35, 40, and 50 K in Figs. 3(b) and 3(c). In Fig. 3(b), we show the PL intensities of the split mode S at a pump level where both branches are lasing. Because of the large emission from the cavity modes, individual QD emission lines can no longer be identified; however, we mark the emission states present under weak excitation [see Fig. 3(a)]. In Fig. 3(c), the lasing threshold of the left branch of mode S is approximately 3 times lower at 50 K than its threshold at 40 K. At 50K, when the pump power is increased so as to pass through the threshold of the left branch, the ratio of integrated intensities of the left-to-right branches changes from 0.2 to 1.6. We explained this by the selective coupling of the QD emission state A with the left branch of the mode. Similarly, at 35 K, emission line D is closely aligned with the short wavelength branch of mode S, and the threshold is also significantly reduced with respect to 40 K. The threshold values as a function of temperature are summarized

in Fig. 3(d). We observe an average of approximately 3 times reduction in threshold when a QD state is aligned with the cavity mode.

We have shown a solid-state laser in which a single emitter, here a single QD state, plays a significant role. Effects due to isolated emitters are seen below and at threshold. Below threshold the initial broadening of the cavity mode is attributed to QD state broadening. When a single QD emission line is tuned to the resonance, the threshold is decreased by a factor of approximately 3. However, under many conditions the cavity lases even though no emitter emission is observed on resonance, as was recently observed in Ref. [23]. To achieve single state lasing the processes associated with the loss must be suppressed and more efficient lasing via the single-emitter state (i.e., higher oscillator strength and higher Q), must be implemented.

We thank Y. Yamamoto for fruitful discussions and use of equipment, and B. Zhang for MBE assistance. Z. G. X. thanks J. S. Harris for advice and encouragement. S. G. acknowledges the Alexander von Humboldt Foundation for financial support.

* Electronic address: glenn.solomon@nist.gov

- [1] D. Meschede, H. Walther, and G. Müller, *Phys. Rev. Lett.* **54**, 551 (1985).
- [2] K. An, J. J. Childs, R. R. Dasari, and M. S. Feld, *Phys. Rev. Lett.* **73**, 3375 (1994).
- [3] J. McKeever *et al.*, *Nature (London)* **425**, 268 (2003).
- [4] B. Lev *et al.*, *Nanotechnology* **15**, S556 (2004).
- [5] Y. Arakawa and H. Sasaki, *Appl. Phys. Lett.* **40**, 939 (1982).
- [6] N. Kirkstaedter *et al.*, *Electron. Lett.* **30**, 1416 (1994).
- [7] H. Cao *et al.*, *Appl. Phys. Lett.* **76**, 3519 (2000).
- [8] P. Michler *et al.*, *Appl. Phys. Lett.* **77**, 184 (2000).
- [9] Z. G. Xie and G. S. Solomon, *Appl. Phys. Lett.* **87**, 093106 (2005).
- [10] Z. Xie, W. Fang, H. Cao, and G. S. Solomon, *J. Cryst. Growth* **278**, 342 (2005).
- [11] A. Badolato *et al.*, *Science* **308**, 1158 (2005).
- [12] G. S. Solomon, M. Pelton, and Y. Yamamoto, *Phys. Rev. Lett.* **86**, 3903 (2001).
- [13] A. Kiraz, *et al.*, *Appl. Phys. Lett.* **78**, 3932 (2001).
- [14] O. Painter *et al.*, *Science* **284**, 1819 (1999).
- [15] J. P. Reithmaier *et al.*, *Nature (London)* **432**, 197 (2004).
- [16] E. Peter *et al.*, *Phys. Rev. Lett.* **95**, 067401 (2005).
- [17] T. Yoshie *et al.*, *Nature (London)* **432**, 200 (2004).
- [18] B.-S. Song, S. Noda, T. Asano, and Y. Akahane, *Nat. Mater.* **4**, 207 (2005).
- [19] J. Hendrickson *et al.*, *Phys. Rev. B* **72**, 193303 (2005).
- [20] G. Björk and Y. Yamamoto, *Phys. Rev. A* **50**, 1675 (1994).
- [21] R. Jin *et al.*, *Phys. Rev. A* **49**, 4038 (1994).
- [22] P. R. Rice and H. J. Carmichael, *Phys. Rev. A* **50**, 4318 (1994).
- [23] S. Strauf *et al.*, *Phys. Rev. Lett.* **96**, 127404 (2006).
- [24] S. Stuffer, P. Ester, A. Zrenner, and M. Bichler, *Appl. Phys. Lett.* **85**, 4202 (2004).